CHAPTER 85

EXPERIMENTAL VERIFICATION OF GROYNE THEORY

by

C.H. Hulsbergen[1], W.T. Bakker[2] and G. van Bochove[3]

1 Abstract. In order to check the results of Bakker's theory [1], [2] concerning the influence of groynes on a sandy beach, a comparison is made with experimental results obtained in model tests performed in the Delft Hydraulics Laboratory [3] , and in the Laboratorio Nacional de Engenharia Civil, Portugal [4] . The theory gives the bathymetric development in terms of a set of two schematized contour lines, representing the onshore and offshore parts of the model where longshore sand transport occurs. As input in the theory the characteristics of the undisturbed sand transport should be known, i.e. without groynes. This is achieved by computing the longshore sand transport acoording to Bijker's method [5] and the transverse sand transport according to Swart's method [6], starting from the hydraulic conditions as measured in the model without groynes. In order to make a comparison with the theoretical lines, the bathymetric development as measured in the model with groynes is also schematized to a set of two contour lines. In some cases the result is quite good, whereas in other conditions the theory does not even show the right trend; see [7] for details. Possible causes are discussed, and shortcomings of the model as well as of the theory are mentioned.

2 Theory. For details of the theory reference is made to [1] and [2]. Only a few basic assumptions and limitations are mentioned here. The theoretical approach may be summarized as follows:

a) The coastal profile is schematized according to Fig. 1 The active zone of the profile, i.e. from an upper dune erosion level down to a depth where relevant changes are no longer significant, is split into two layers with a thickness D1 and D2. Each layer extends seaward from a common base line over a certain distance, L1 and L2, respectively. The area of the schematized step-type cross-section is equal to the area of the actual profile. The elevation of the horizontal interface is defined by the point where the seaward toe of the groyne intersects the actual beach profile. In top view, the two layers appear as a set of two lines, referred to as beach-line and foreshore-line respectively (Fig. 2).

b) The rates of littoral drift S1 and S2 along beach and foreshore each have a linear relationship with the local angle of wave incidence:

$$S1 = So1 - s1 \frac{\partial y1}{\partial x} \quad \text{and} \quad S2 = So2 - s2 \frac{\partial y2}{\partial x} \qquad (1)$$

where So1 (So2) = undisturbed longshore transport along beach-line (foreshore-line); s1 (s2) = factor of proportionality; $\partial y1/\partial x$ ($\partial y2/\partial x$) = local angle between beach-line (foreshore-line) and base line.

c) The transport Sy perpendicular to the coast, taking place between the beach and the foreshore, depends on the steepness of the (schematized) profile. Whenever the distance L2 - L1 is smaller than a certain equilibrium distance W, the profile is too steep, causing a seaward transport. In the opposite case there is a landward transport (Fig. 2):

---

1 Delft Hydraulics Laboratory, Project Engineer.
2 Rijkswaterstaat, Head Study Department Flushing.
3 Rijkswaterstaat, Coastal Research Engineer.

$$Sy = \underline{sy} \left[\underline{W} - (L2 - L1) \right] \qquad (2)$$

where sy is a factor of proportionality.

In (1) and (2) the underlined terms are "coastal constants", which controll both the time scale and the geometric scale of the coastal development, and which have to be determined in order to achieve quantitative results. Here, the "coastal constants" are quantified from:

- experiments without groynes
- Bijker's theory [5] for longshore transport
- Swart's theory [6] for perpendicular transport.

d) Continuity of the sand volume is specified by

$$-\frac{dS1}{dx} - Sy = D1 \frac{\partial y1}{\partial t} \quad \text{and} \quad -\frac{dS2}{dx} - Sy = D2 \frac{\partial y2}{\partial t} \qquad (3)$$

e) The main boundary condition is formed by the complete obstruction of that fraction of the littoral drift which moves along the beach-line. Moreover, there is continuity in the location and in the orientation of the foreshore-lines on both sides of every groyne.

A visualization of a typical theoretical result is given in Fig. 3. It gives rise to a few comments. The theory, in its basic form as outlined above, gives only one type of coastal evolution, i.e. a certain amount of accretion upstream and an equal amount of erosion downstream, in a pattern which is basically fixed. That is so, because the hypotheses concerning the sand transport tacitly assume a quite neat and "nicely" behaving breaking wave and longshore current. In fact, the theory is not dealing with any detail of the coastal current system or the sand transport phenomenon. In order to make the theory more realistic, the possibility has been added to include such influences as rip-currents, stream refraction, and diffraction. However, exept for a single case (Chapter 4), these options have not been used here, because their application presumes detailed a priori knowledge about the current pattern, which was not available. For this reason Chapter 3 gives the experimental results against the background of the theory in its basic form, as represented by Fig. 3. The procedure for this comparison is outlined in Fig. 4.

3 Experiments in Delft Hydraulics Laboratory

3.1 Model facility and test procedure

The lay-out of the model basin is given in Fig. 5. A large amount of various conditions were installed, details of which are extensively discussed in [3]. As bed material dune sand was used with ρ = 2650 kg m^{-3} and D_m = 0.220 mm. Either 0, 1 or 3 impermeable groynes were present, with their crests well above the water level, with rough 1:1 slopes and aligned perpendicularly to the coast. The spacing was 6 m and their length so that they obstructed the longshore current partly or completely. The regular waves had a period of 1.55 s or 1.15 s, and a height between 0.07 m and 0.14 m. Depending on the wave steepness and the local beach slope, either spilling or plunging breakers occurred, under an angle of appr. 5° with the shore line. Water and sand were fed upstream and caught downstream in order to represent an inifinitely long, straight beach.

In short, the procedure was to try and establish a dynamic equilibrium along a straight beach without groynes, and to assess meanwhile the development of the wave heights, the current velocity, the morphology and the trapped sand distribution. Then, after adding a groyne system, the new hydraulic and bathymetric development were recorded and subsequently compared with the theory. Here only a limited, though typical, selection of the numerous test results is presented, while in Chapter 5 a discussion is given, making use of some more selected measuring

data which are deemed useful for a good interpretation of the results.

3.2 Tests with a single groyne.

Representative as a "good" tests is T22, where the main conditions were: wave height 0.075 m, wave period 1.55 s, water depth 0.38 m in front of the wave generators. The average rate of sand nourishment was 71 dm^3hr^{-1}, while 55 dm^3hr^{-1} was caught in the traps. The rate of water supply was constant at 30 $dm^3\ s^{-1}$ in order to feed the longshore current. The groyne extended seaward to 4.2 m, whereas the waves broke at appr. 3.5 m. Fig. 6 and 7 depict the beach, looking upstream, after 0.5 hr and 50 hrs. They show a quite regular accretion upstream, and erosion downstream of the groyne. This is also represented by Fig. 8, a difference chart displaying the extent and the locations of erosion and accretion during the 50 hrs of the test. In an attempt to monitor the actual longshore sand transport by local measurements, the wave height and the longshore current distribution were frequently measured in sections perpendicular to the shore. These data, together with the local depth and the bed material characteristics, are enough to compute the longshore sand transport according to Bijker. Examples are given in Figs. 9 and 10 for a section 8 m upstream of the groyne, and at the groyne itself, respectively. The obvious decrease of the longshore sand transport capacity is in good accordance with the observed accretion of the beach. Fig. 11 shows both rates of longshore sand transport in the course of time. Typical accreting and eroding coastal profiles are given in Figs. 12 and 13, respectively, the latter together with the distribution of the longshore sand transport as caught in the sand traps.

From Bijker's and Swart's theories, together with the appropriate data from the experiment, the following quantities were derived for application of the theory:
upper level of beach : 0.51 m
elevation of interface : 0.24 m
lower level of foreshore: 0.18 m
} with respect to the level of the wave generator floor.
$So1 = 87\ dm^3hr^{-1}$, $s1 = 994\ dm^3hr^{-1}$, $So2 = 29\ dm^3hr^{-1}$, $s2 = 332\ dm^3hr^{-1}$, $W = 7.62$ m
$sy = 0.0338\ dm\ hr^{-1}$.

The resulting schematized beach- and foreshore-lines for 0.10 and 50 hrs are given in Fig. 14, together with the comparable theoretical lines. The fit is quite good, especially for the beach-lines. It is thought that this favourable result was reached under the influence of an extraordinarily regular breaker type (plunging), which was accompanied by a very regular longshore current. Moreover, the groyne interrupted the longshore current almost entirely, thus obstructing the longshore transport of sand to a great extent.

Another test with a single groyne, T18, contrasted sharply with the above result. Its main conditions were: wave height 0.10 m, wave period 1.55 s, water depth 0.38 m in front of the wave generators, average rate of sand nourishment 88 dm^3hr^{-1}, while 106 dm^3hr^{-1} was caught in the traps. The water discharge was constant at 55 $dm^3\ s^{-1}$. In Fig. 15 the contours after 60 hrs are shown, where the attention is drawn to the clear accretion, but this time downstream of the groyne. Locally even a new beach line appeared seaward of the original one. The development can be followed on Figs. 16 and 17, where difference charts of 0-20 hrs and 20-60 hrs are showing how the bulk of the longshore sand transport moved around the groyne in two stages. In the intermediate stage the maximum accretion amounted to 20 cm at some distance downstream and seaward of the head of the groyne. After 20 hrs the bulk of this sand deposit was removed and shifted in shoreward direction, and somewhat more downstream. Fig. 18 shows that neither the upstream nor the downstream overall profile was subject to large changes. It also points towards a possible reason for the remarkable developments encountered here: the trapped sand distribution, averaged over 60 hrs, indicates that the groyne could hardly be expected to stop the longshore transport. However, the average trapped sand distribution in the preceeding test T17 (without groyne), was used

to design this groyne length such that it would stop approximately 50% of the existing longshore sand transport.
After the above explanation it is not surprising that the experimental results are not well covered by the theoretical beach- and foreshore-lines (Fig. 19), which are based on the following data:
upper level of beach : 0.46 m
elevation of interface : 0.235 m
lower level of foreshore: 0.06 m
} with respect to the level of the wave generator floor.
So1 = 73.5 dm^3hr^{-1}, s1 = 840 dm^3hr^{-1}, So2 = 65 dm^3hr^{-1}, s2 = 743 dm^3hr^{-1}, W = 10.08 m, sy = 0.029 dm hr^{-1}.

The impression exists from various observations (see also Chapter 5) that secondary wave formation, caused by the bar at a distance of 11 m (Fig. 18), may have played an important part in re-establishing the original coastal profile after 20 hrs. It is felt that this type of secondary waves has an important influence on coastal profile dynamics.

3.3 Tests with a row of three groynes.
In Fig. 20 the contours after 50 hrs of test T23 with three groynes are presented. The conditions were: wave height 0.075 m, wave period 1.55 s, water depth 0.38 m in front of the wave generators. The average rate of sand nourishment was 44 dm^3hr^{-1}, while 27 dm^3hr^{-1} was caught in the traps. The average rate of water supply was 25 dm^3s^{-1}. The groynes extended to 3.7 m. Until 20 hrs a plunging breaker occurred at appr. 3.7 m, whereas later on the spilling type dominated, with variations in breaker location. In Fig. 21 a clear rhythmic behaviour is revealed by the difference chart, both in longshore direction (as caused by the groynes) and in perpendicular direction (as caused by an overall coastal profile development). The various quantities with respect to the theoretical computations are:
upper level of beach : 0.51 m
elevation of interface : 0.255 m
lower level of foreshore: 0.160 m
} with respect to the level of the wave generator floor.
So1 = 87 dm^3hr^{-1}, s1 = 995 dm^3hr^{-1}, So2 = 29 dm^3hr^{-1}, s2 = 331 dm^3hr^{-1}, W = 8.10 m sy = 0.032 dm hr^{-1}.

Fig. 22, displaying the experimental and theoretical lines representing the beach and the foreshore, reveals a reasonable equality as far as the beach is concerned. However, large deviations occur in the foreshore, where the typical rhythmic variations are not found back in the theory.

Test T34 had unusual conditions in so far that the water level fluctuated in a one-hour cycle 0.025 m plus and minus the average of 0.38 m above the wave generator floor. This was done in order to shift also the type and the location of the breaking waves, in an attempt to avoid rip-current formation at fixed locations. The other conditions were: wave height 0.115 m, wave period 1.15 s, average rate of caught sand 74 dm^3hr^{-1}. The rate of sand nourishment was constant at 70 dm^3hr^{-1}, and the rate of flow was constant at 50 dm^3s^{-1}. The groynes extended to 3.27 m, whereas the breaker location varied widely during the test.

The quantities for the theoretical analysis were:
upper level of beach : 0.49 m
elevation of interface : 0.27 m
lower level of foreshore: -0.01 m
} with respect to the level of the wave generator floor.
So1 = 32.4 dm^3hr^{-1}, s1 = 370 dm^3hr^{-1}, So2 = 35.6 dm^3hr^{-1}, s2 = 407 dm^3hr^{-1}, W = 8.11 m, sy = 0.108 dm hr^{-1}.

The result was not much better than that of test T23, as can be seen on Figs. 23, 24 and 25. Fig. 24 is a special chart, displaying the difference between test T34 and test T33 (without groynes but further with exactly the same conditions as T34) after 30 hrs. The pattern of alternating erosion and accretion between the groynes is opposite to what should be expected from the theory. This is most probably caused by an intricate and unstable pattern of currents, stagnation areas, rip currents and regions of lower and higher waves.

4 Experiments in Laboratorio Nacional de Engenharia Civil.

4.1 Model facility and test conditions.

Reference is made to [4] for details. Fig. 26 shows the lay-out of the model. A convex beach profile of pumice-stone (ρ = 1670 kg m^{-3}, D_m = 1.25 mm) was molded between two rockfill groynes E1 and E3. These groynes had 2:1 absorbent slopes and acted as training walls for the beach. A smaller groyne E2 in between with steep 1:5 slopes completely obstructed the littoral drift. The waves were 0.02 m high, had a period of 1 s and were generated under an angle of 20° in a water depth of 0.40 m.

4.2 Test results and theoretical beach lines.

Various beach line positions were recorded during the 35 hr test, as presented in Fig. 27. These are compared to theoretical lines, which were determined as follows [8]. The active profile was schematized to a single beach line, because perpendicular transport across the 0.063 m depth contour was assumed negligible. This depth is twice the breaker depth as calculated for straight, parallel depth contours. Diffraction calculations were performed in the deeper, horizontal part of the basin, whereafter refraction was calculated up to the 0.063 m contour line, again assuming straight and parallel depth contour lines, remaining so during the whole test. The resulting values for the wave height H1 and the angle of wave attack ϕ1 at the 0.063 m depth contour are given in Fig. 28.

The final position of the beach is now assumed to be defined by ϕ1 and H1 in a first approximation. By ϕ1 alone, the final beach line is determined by being parallel to the local wave crest as defined by ϕ1, because only then the net transport along any part of the beach is equal to zero. By H1 alone on the other hand, differences in wave set-up will develop, causing a varying longshore current velocity V1 along the beach, where V1 is a function of various parameters among which the beach line orientation [9]. By putting V1 equal to zero, the final beach alignment is found. After adding the partial solutions for H1 and ϕ1, the final coastline is found as Yo in Fig. 29. By comparing this line to the experimental 35 hrs-line in Fig. 27, some differences can be found:

- In the experiment a certain amount of material does disappear into deeper water. Because Barcelo reports a rip-current near groyne E2, the theoretical line is adapted by taking a sand transporting rip-current into account near E2 with an adequate transport capacity. This will at the same time increase the theoretical beach line angle near groyne E2, bringing it closer to the measured position.
- Differences near groyne E1 are likely to be caused by a very low transport capacity in the model, whereas in the calculation no critical velocity for beginning of movement is used.

For the calculation of the coastline after 1, 4, 7, 15 and 35 hrs the dynamic equation is used (with sy = 0), together with equation (1). Relevant quantitative parameters are: $S_{ripcurrent}$ = 3.4 dm^3hr^{-1}, Sol = 27.8 dm^3hr^{-1} acc. to Barcelo, s1 = 150 dm^3hr^{-1}. The resulting theoretical lines are given in Fig. 29; they fit quite well with the experimental lines of Fig. 27.

5 Discussion of the results. The above examples are typical in so far that they indicate the rather large variation in the ability of the theory to fit with the experimental results. One should not be too surprised, in view of the wide deviations which were often present in the actual experimental conditions, as compared to the ideal conditions which were (tacitly) assumed in the theory. The main causes of deviation are discussed below.

- Variations in wave height as measured in cross-sections very close to each other, were frequently noted and were judged to have a strong negative effect on the homogeneous conditions sought. Fig. 30 shows a rather dramatic example, in which the wave height variations are at least partly due to the varying bed profiles. Of course there exists a strong mutual interaction between wave behaviour and coastal profile development.
- An example of the progressively deteriorating homogeneity in longshore direction of the coastal profiles is given in Fig. 31. It shows the envelopes of all cross-sections after 10, 30 and 50 hrs in test T19 (without groyne).
- An effect, and simultaneously a cause, of the above mentioned non-homogeneity is present in the chaotic current pattern in the same test, as presented in Fig. 32. This test, too, began with a nice homogeneous and steady longshore current.
- Apart from being non-homogeneous, the current pattern was unsteady, as is shown in Fig. 33. It gives values of the longshore current in test T25, measured in two points 1 m apart perpendicular to the coast. The measurements were performed by timing floats over a distance of 1 m.
- Secondary waves were present under certain conditions. Apart from those, generated by the sinusoïdally moving wave board [10], also secondary waves were generated while the regular waves passed over a large bar without breaking. In this respect it is interesting to not that Byrne [11] reports the same wave behaviour (long regular swell conditions) in the prototype (Fig. 34). Fig. 35 presents a coastal profile of test T19, with a bar and with the wave height over it; the wave breaks only at a distance of appr. 5 m. The respective wave forms as shown in Fig. 36 clearly show the presence of secondary waves (with period T/2) which are overtaken gradually by the faster main waves. Their presence has undoubtedly a large influence on the perpendicular sand transport [10], and further on the type of breaking and the kinematic results thereof. It is felt that the presence of those secondary waves can have a dominating effect on the formation and the stability of coastal profiles.
- The pair of Fig. 37 and 38 illustrates the strong relationship between secondary waves, bar formation, type of breaker, and subsequently the rate and distribution of the longshore transport. The conversion of the breaker type from spilling to plunging was in very good agreement with Galvin's results as far as the influence of the seaward slope of the breaker bar is concerned [12]. After this conversion the rate of longshore transport was appr. three times as large as before, and much more concentrated.
- The most obvious visible result of the increasingly non-homogeneous conditions in many tests was the formations of beach cusps. Both small (Fig. 39) and large (Fig. 40) examples have been recorded. It goes without saying that this is most unwelcome in tests which are ment to verify the effect of groynes on a sandy beach. Fortunately, the presence of a groyne appeared to induce a more stable condition, in which the cusp formation was partly suppressed.

6 Conclusions. The conclusions which follow from these tests and their comparison with the theory can be summarized as follows.

- The theory is good in cases with a stable, neat, and well defined longshore current system, and if the groyne(s) intercept a substantial part of the longshore sand transport.
- In other, more complex systems, the theory in its present form is not adequate on a forecast basis. However, if the current pattern is well enough defined and specified, the theoretical result may be improved by taking into consideration the effects of stream refraction, diffraction, and rip-currents.
- The coastal current system should be studied in more detail in order to improve the theory of Bakker.

REFERENCES

1 BAKKER, W.T., The dynamics of a coast with a groyne system. 11th Conf. on Coastal Engineering, Ch. 31, London 1968
2 BAKKER, W.T., KLEIN BRETELER, E.H.J. and ROOS, A., The dynamics of a coast with a groyne system. 12th Conf. on Coastal Engineering, Ch. 64, Washington 1970
3 DELFT HYDRAULICS LABORATORY, The influence of groynes on the coast, Report M 918 part I (experiments) March 1976 (in Dutch)
4 BARCELO, J.P., Experimental study of the hydraulic behaviour of groyne systems. 11th Conf. on Coastal Engineering, Ch. 13, London 1968
5 BIJKER, E.W., Longshore transport computations. Proc. A.S.C.E., vol. 97, WW 4, pp. 687-701, November 1971
6 SWART, D.H., A schematization of onshore-offshore transport. 14th Conf. on Coastal Engineering, Chapter 51, Copenhagen 1974
7 DELFT HYDRAULICS LABORATORY, Comparison of theoretical and experimental coast lines, Report M 918 part III, 1976 (in Dutch)
8 BOCHOVE, G. van, Elaborations of a model test conducted by Barcelo. Memo 72-21 of Rijkswaterstaat, Dir. Water Management and Water Movements, Section Coastal Research, The Hague 1972
9 BAKKER, W.T., The influence of longshore variation of the wave height on the littoral current. Study-Report WWK 71-19 of Rijkswaterstaat, Dir. Water Management and Water Movements, Section Coastal Research, The Hague 1971
10 HULSBERGEN, C.H., Origin, effect and suppression of secondary waves. 14th Conf. on Coastal Engineering, Chapter 22, Copenhagen 1974
11 BYRNE, R.J., Field occurrences of induced multiple gravity waves. Journ. of Geoph. Res., vol. 74, 1969, no. 10, May 15, pp. 2590-2596
12 GALVIN, C.J., Classification of breaking waves on three laboratory beaches. C.E.R.C. Res. Divn, 1967.

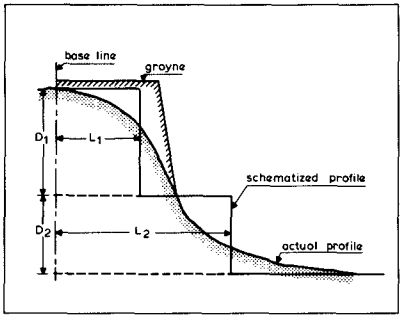

Fig. 1 Schematization of coastal profile

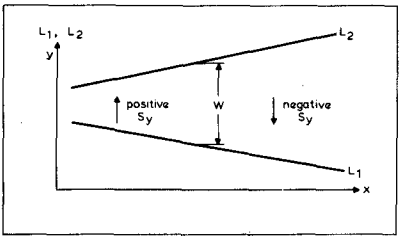

Fig. 2 Top view of schematized coast lines

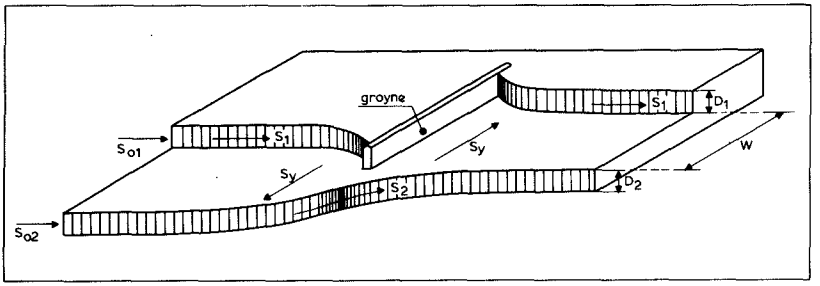

Fig. 3 Visualization of theoretical coast

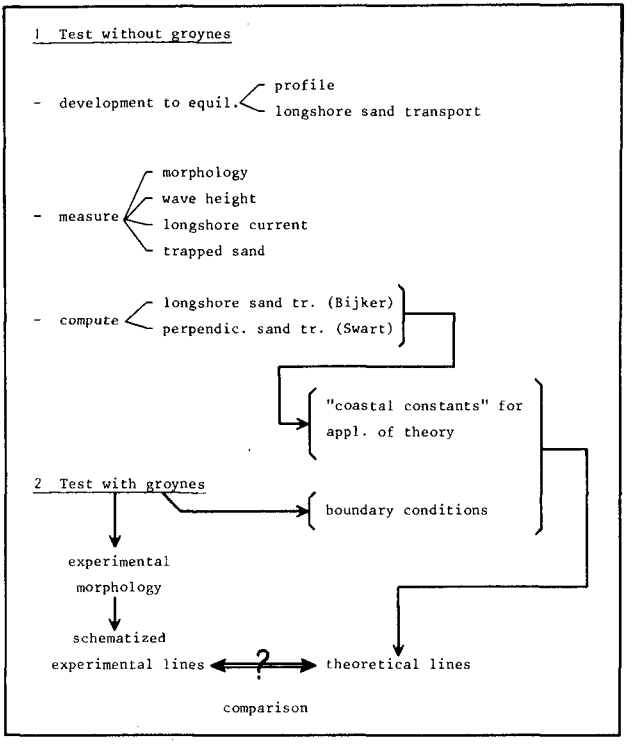

Fig. 4 Procedure of verification

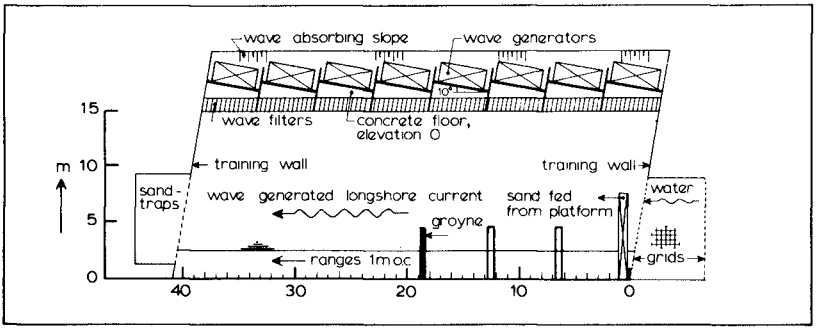

Fig. 5 Lay-out of model facility

Fig. 6 Test T22 after 0.30 hrs.

Fig. 7 Test T22 after 50 hrs.

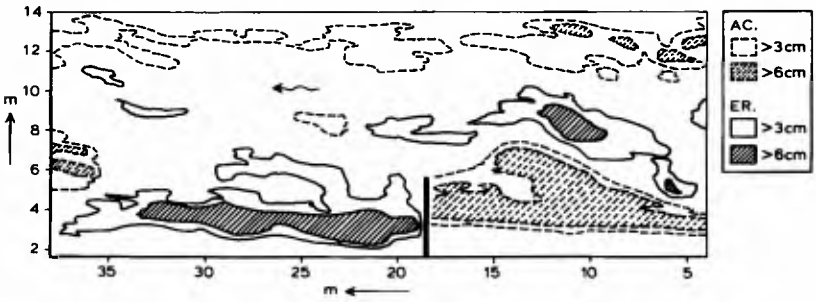

Fig. 8 Test T22, difference chart 0-50 hrs.

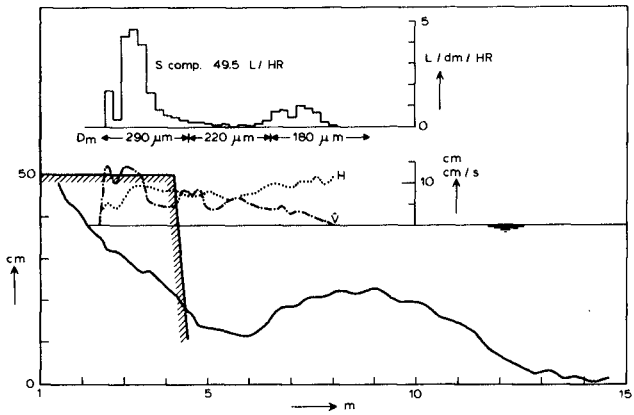

Fig. 9 Test T22, 8 m upstream of groyne after 3 hrs.

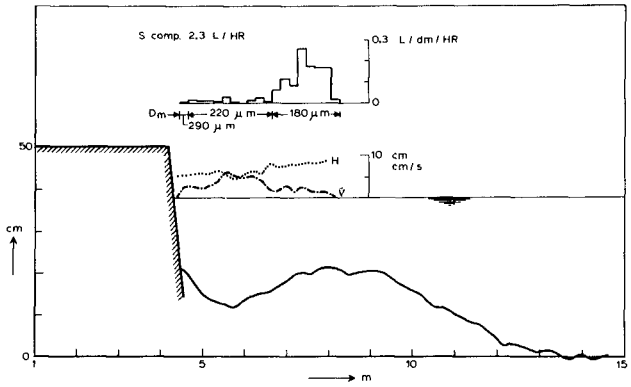

Fig. 10 Test T22, at groyne after 4 hrs.

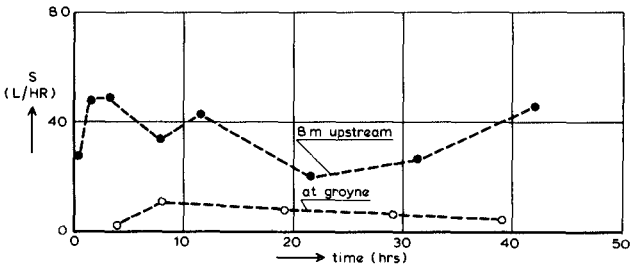

Fig. 11 Test T22, longshore transport according to Bijker

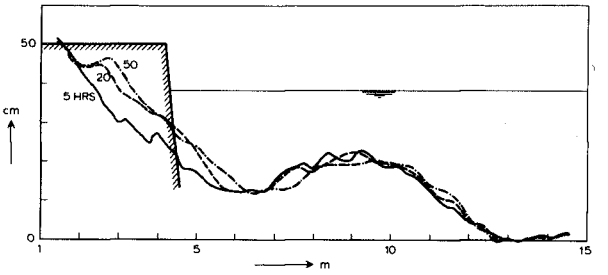

Fig. 12 Test T22, 3.5 m upstream of groyne

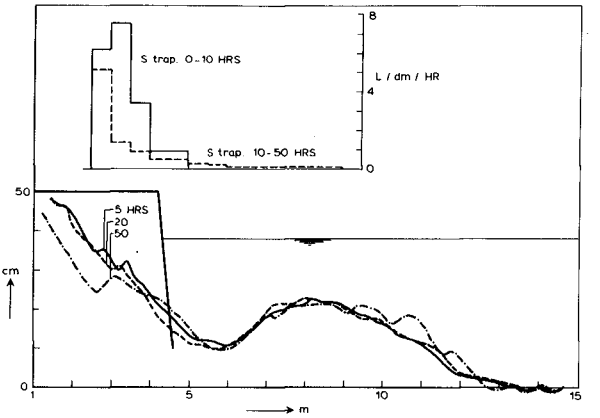

Fig. 13 Test T22, 3.5 m downstream of groyne

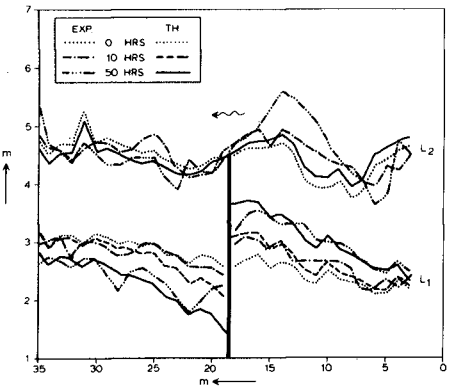

Fig. 14 Test T22, comparison of beach- and foreshore-lines

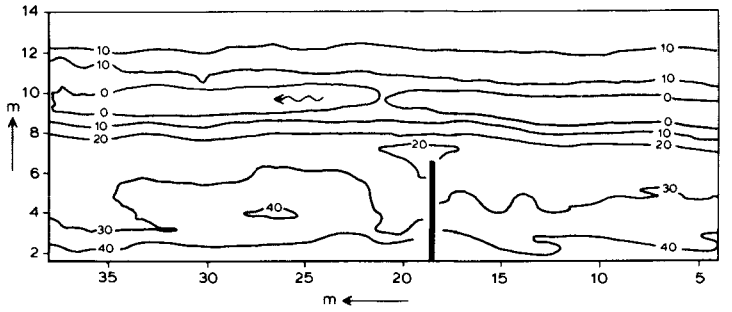

Fig. 15 Test T18, 60 hrs, contours in cm above model datum

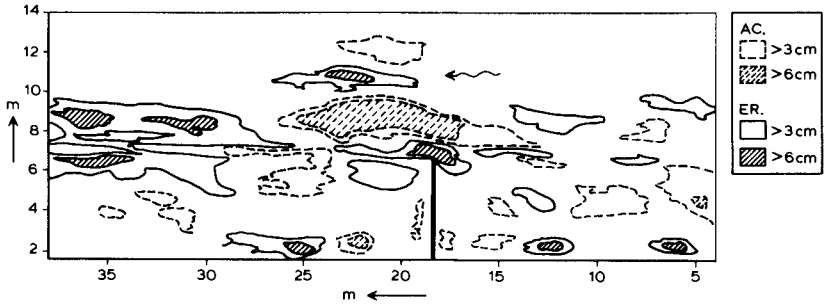

Fig. 16 Test T18, difference chart 0-20 hrs.

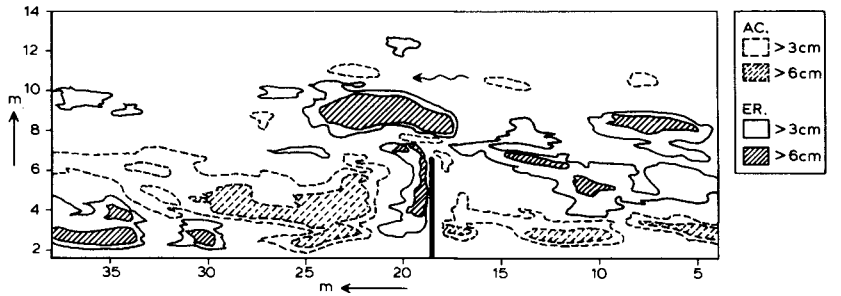

Fig. 17 Test T18, difference chart 20-60 hrs.

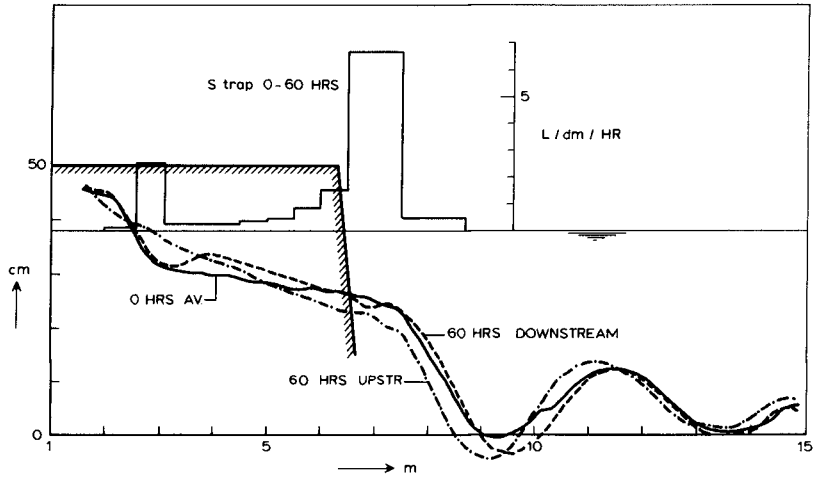

Fig. 18 Test T18, average upstream and downstream profiles

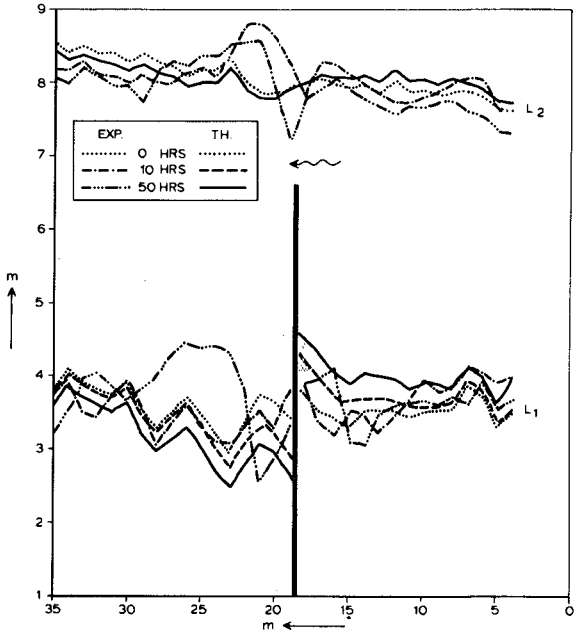

Fig. 19 Test T18, comparison of beach- and foreshore-lines

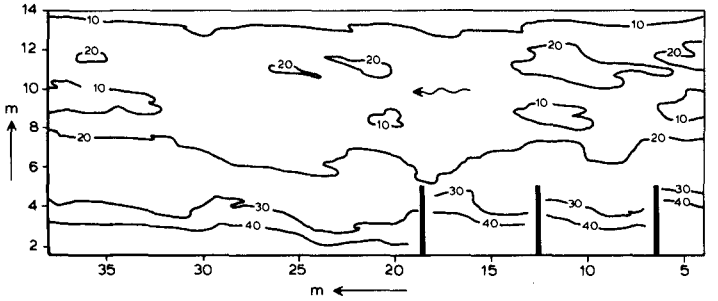

Fig. 20 Test T23, 50 hrs, contours in cm above model datum

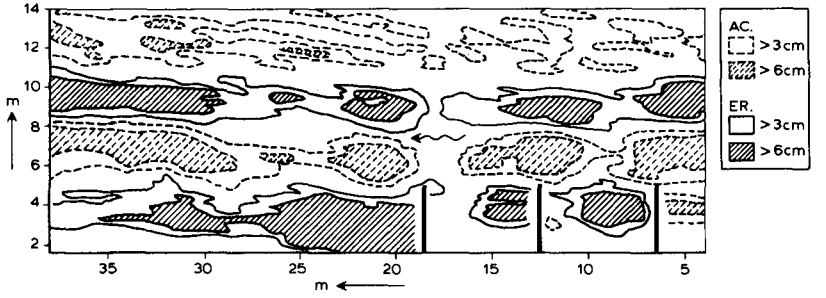

Fig. 21 Test T23, difference chart 0-50 hrs.

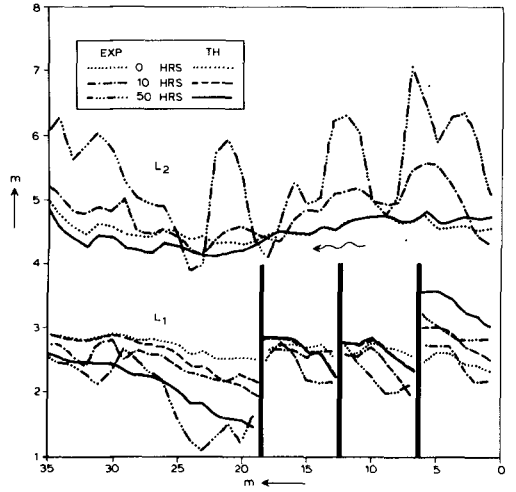

Fig. 22 Test T23, comparison of beach- and foreshore-lines

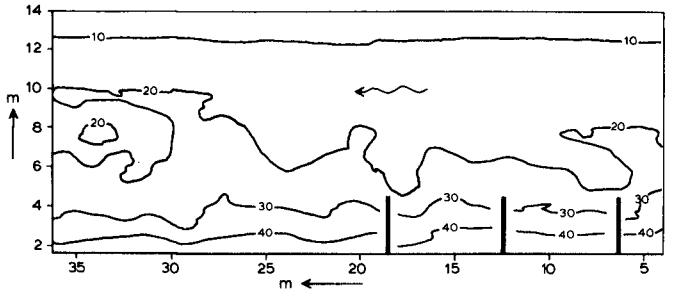

Fig. 23 Test T34, 45 hrs, contours in cm above model datum

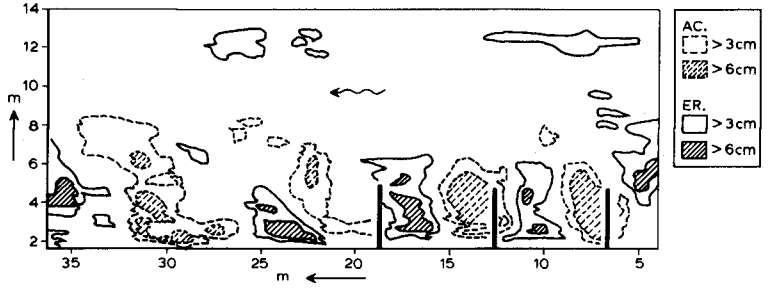

Fig. 24 Test T33/34, groyne effect 30 hrs.

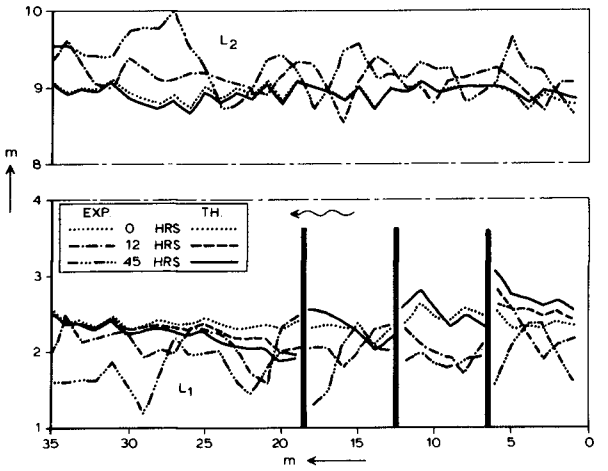

Fig. 25 T34, comparison of beach- and foreshore-lines

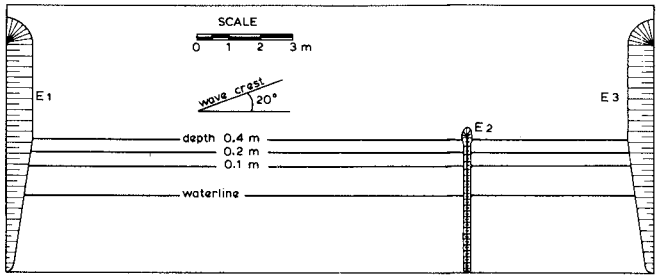

Fig. 26 LNEC test, lay-out of model basin

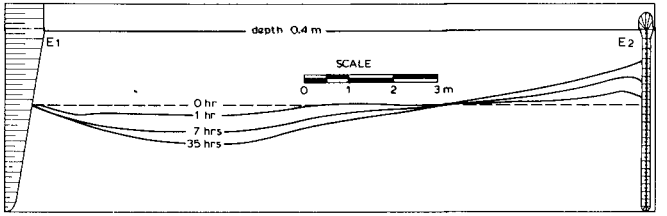

Fig. 27 LNEC test, experimental beach-lines

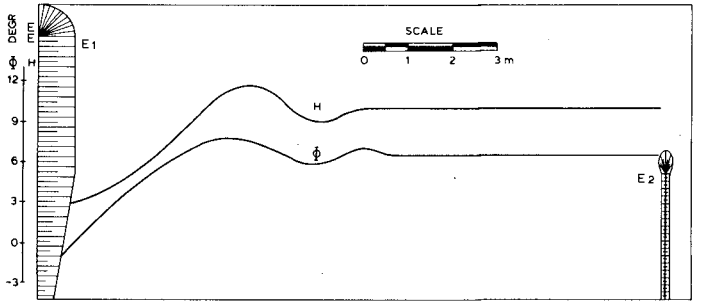

Fig. 28 LNEC test, wave height and angle of wave incidence

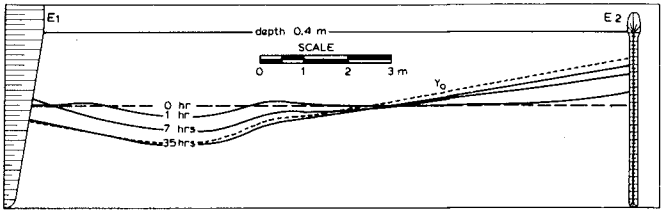

Fig. 29 LNEC test, theoretical beach-lines

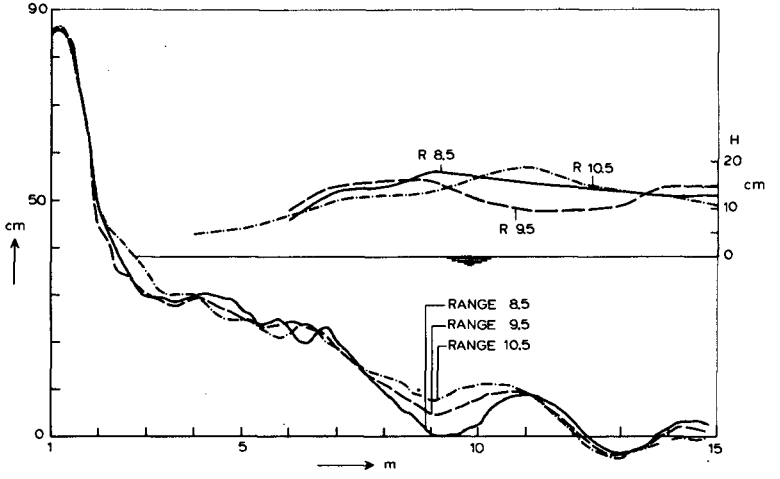

Fig. 30 Test T2, variety in beach profiles and wave heights

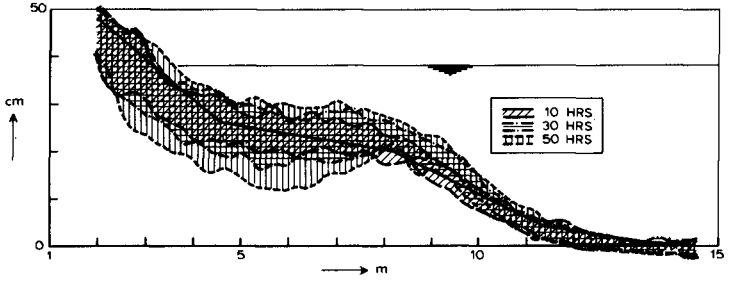

Fig. 31 Test T19, envelopes of beach profiles

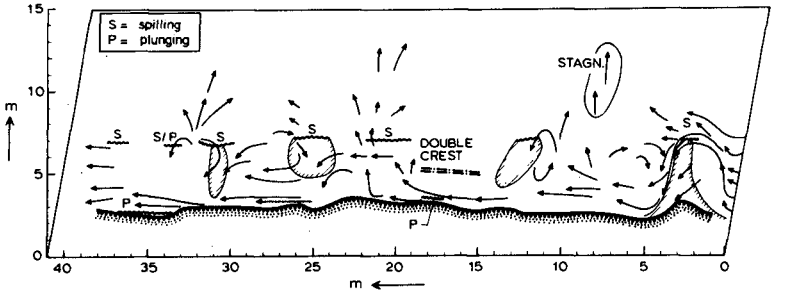

Fig. 32 Test T19, current pattern 77 hrs.

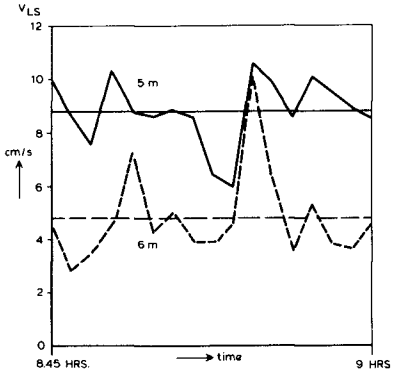

Fig. 33 Test T25, unsteadiness in longshore current velocity

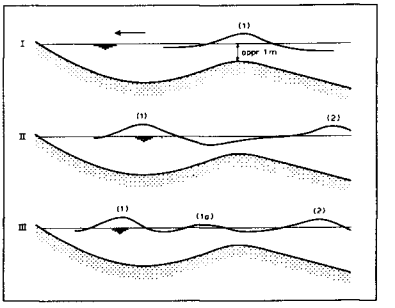

Fig. 34 Prototype observation of induced multiple gravity waves (after Byrne)

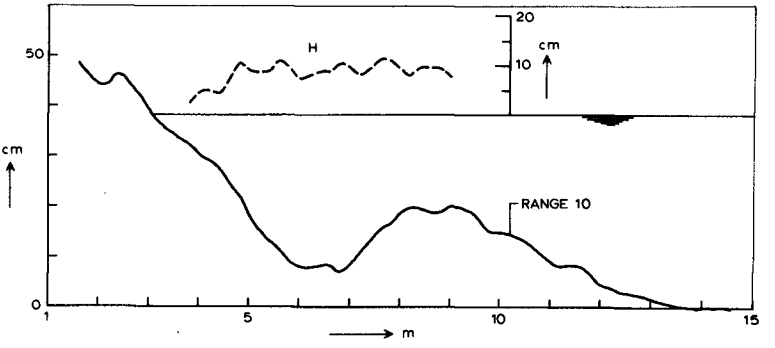

Fig. 35 Test T19, 105 hrs, bar profile and wave height

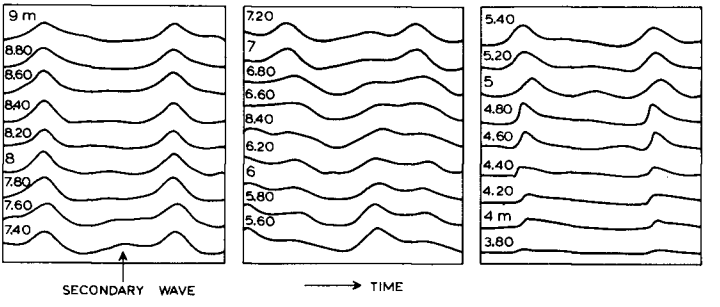

Fig. 36 Test T19, wave forms over bar profile from Fig. 35

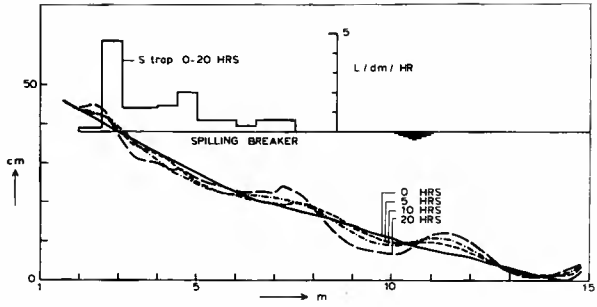

Fig. 37 Test T17, spilling breaker conditions 0-20 hrs.

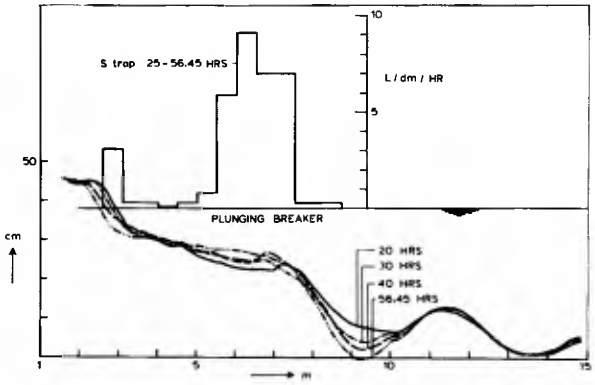

Fig. 38 Test T17, plunging breaker conditions 20-56.45 hrs.

Fig. 39 Test T19, small scale beach cusps

Fig. 40 Test T27, large scale beach cusps